

1 **Pollen, biomarker and stable isotope evidence of late Quaternary**  
2 **environmental change at Lake McKenzie, southeast Queensland**

3

4 Pia Atahan<sup>a,b,\*</sup>, Henk Heijnis<sup>a</sup>, John Dodson<sup>a</sup>, Kliti Grice<sup>b</sup>, Pierre Le Métayer<sup>b</sup>, Kathryn Taffs<sup>c</sup>, Sarah  
5 Hembrow<sup>c</sup>, Martijn Woltering<sup>b</sup>, Atun Zawadzki<sup>a</sup>

6 <sup>a</sup> Institute for Environmental Research, Australian Nuclear Science and Technology Organisation,  
7 Sydney, Locked Bag 2001, Kirrawee DC, NSW 2232, Australia

8 <sup>b</sup> WA-Organic and Isotope Geochemistry Centre, Department of Chemistry, Curtin University, GPO  
9 Box U1987, Perth, WA 6845, Australia

10 <sup>c</sup> Southern Cross Geoscience and School of Environment, Science and Engineering, Southern Cross  
11 University, PO Box 157, Lismore NSW 2480, Australia

12

13 \* Corresponding author: email address: [pia.atahan@ansto.gov.au](mailto:pia.atahan@ansto.gov.au); telephone: +61 2 9717 7261

14

15

16 **Abstract**

17 Unravelling links between climate change and vegetation response during the Quaternary is  
18 important if the climate-environment interactions of modern systems are to be fully understood.  
19 Using a sediment core from Lake McKenzie, Fraser Island, we reconstruct changes in the lake  
20 ecosystem and surrounding vegetation over the last ca. 36.9 cal kyr. Evidence is drawn from multiple  
21 sources, including pollen, micro-charcoal, biomarker and stable isotope (C and N) analyses, and is  
22 used to gain a better understanding of the nature and timing of past ecological changes that have  
23 occurred at the site. The glacial period of the record, from ca. 36.9-18.3 cal kyr BP, is characterised

24 by an increased abundance of plants of the aquatic and littoral zone, indicating lower lake water  
25 levels. High abundance of biomarkers and microfossils of the colonial green alga *Botryococcus* occur  
26 at this time and include large variation in individual botryococcene  $\delta^{13}\text{C}$  values. A slowing or ceasing  
27 of sediment accumulation occurs during the time period from ca. 18.3-14.0 cal kyr BP. By around  
28 14.0 cal kyr BP fire activity in the area was reduced, as was abundance of littoral plants and  
29 terrestrial herbs, suggesting wetter conditions from that time. The Lake McKenzie pollen record  
30 conforms to existing records from Fraser Island by containing evidence of a period of reduced  
31 effective precipitation commencing in the mid-Holocene.

32

### 33 **Key words**

34 Quaternary, *Botryococcus*, pollen, palaeoecology, Fraser Island, southeast Queensland

35

### 36 **Introduction**

37 Lake sediment is an important source of information about late Quaternary climate and  
38 environmental change in southeast Queensland, Australia. The region has produced long and high  
39 quality records focused on microfossils (pollen, diatoms and charcoal) and geochemistry, and these  
40 have been used to reconstruct past changes in vegetation, human activity and aeolian sedimentation  
41 (Longmore 1997; Longmore and Heijnis 1999; Donders et al. 2006; McGowan et al. 2008; Barr et al.  
42 2013; Moss et al. 2013). Much of what is known about Quaternary environments in the subtropical  
43 region of Australia has come from lake records on North Stradbroke Island and Fraser Island, and  
44 records from these islands have recently been included in continent-scale climate syntheses  
45 produced by the OZ-INTIMATE project (Petherick et al. 2013; Reeves et al. 2013). Despite this  
46 region's importance in understanding factors driving climate in subtropical Australia, in comparison

47 to temperate regions it has a low density of sediment-based proxy records extending into the last  
48 glacial.

49 This study focuses on reconstructing past environmental change at a lake site on Fraser Island,  
50 using microfossil, biomarker and stable isotope analysis techniques. This study builds on previous  
51 work at the site, using diatom and branched glycerol dialkyl glycerol tetraether (GDGT) distributions  
52 (Hembrow and Taffs 2012; Hembrow et al. 2014; Woltering et al. 2014), and aims to broaden  
53 understanding of past environmental conditions at the site. Some key benefits of including  
54 biomarker and compound specific isotope techniques in studies of Quaternary-aged sediment have  
55 for example been discussed by Bianchi and Canuel (2011), Eglinton and Eglinton (2008) and Sachs et  
56 al. (2007) and importantly include the attainment of otherwise unavailable information about past  
57 isotope reservoirs and presence of organisms not associated with hard fossil remains.

58

## 59 **Site Description**

60 Lake McKenzie is a clear water oligotrophic lake located in an elevated inland area of Fraser Island,  
61 about 7 km from the western coastline (25°26'51" S, 153°03'12" E; Fig. 1). The lake has an area of  
62 about 94 ha, an elevation of 85 m above sea level and lies amongst dunes that reach 150 m in  
63 elevation. The lake is positioned above the regional groundwater table, and its relatively  
64 impermeable base-layer (a B-horizon) restricts downwards percolation of water (Timms 1986;  
65 Longmore 1998). The lake has no inflow or outflow creeks and thus is highly responsive to changes in  
66 precipitation and evaporation. Concentrations of total phosphorus are low (2-5 µg L<sup>-1</sup>), as is pH (4.8 –  
67 5.8), and dominant types of phytoplankton are *Sphaerocystis*, *Oocystis* and *Peridinium* (Bowling  
68 1988; Hadwen et al. 2003). Living *Botryococcus* has not been reported in this lake, although it is  
69 reported in other perched lakes on Fraser Island (Bowling 1988). The lake lies within a national park  
70 that has been largely protected from industrial and residential development.

71 The Fraser Island landmass is composed of Quaternary-aged sand dunes that were formed  
72 progressively during periods of lower sea level (Lees 2006). The climate is subtropical. Rainfall  
73 derives mostly from south-easterly trade winds and tropical cyclones from the north. Mean monthly  
74 rainfall for January and July is respectively around 160 and 90 mm, and mean monthly temperatures  
75 are between 20 and 32°C in January and 12 and 23°C in July (Australian Bureau of Meteorology  
76 2013). Precipitation patterns on Fraser Island are strongly influenced by topography, rainfall is  
77 substantially higher in elevated areas on dune slopes (Longmore 1998)

78 The sandy soils of Fraser Island support a diverse range of vegetation communities, including  
79 heathlands, woodlands, tall eucalypt forest, and closed rainforest. Local water table depth, nutrient  
80 availability, soil salinity and local burning regimes are important influences on the structure and  
81 composition of vegetation communities on the island. Common vegetation communities are  
82 *Eucalyptus signata* - *Banksia wallum* heathland; coastal woodland, sedgeland and swamp; tall  
83 eucalypt forest with *Syncarpia hillii* and *Lophostemon confertus*; and tall closed forest with rainforest  
84 and *E. pilularis* (Ryan 2012). Vegetation on slopes surrounding Lake McKenzie is composed of tall  
85 forest with *E. racemosa*, *E. pilularis*, *E. microcorys*, *E. resinifera* and *Syncarpia hillii*. Dominant plants  
86 of the littoral zone are *Baumea* spp., *Juncus* spp. and *Lepironia articulata* (Ryan 2012).

87

## 88 **Methods**

### 89 **Sampling and Dating**

90 The methods by which the Lake McKenzie cores were sampled and dated has been previously  
91 described by Hembrow et al. (2014) and Woltering et al. (2014). Two adjacent sediment cores were  
92 extracted from the centre of the deepest basin of Lake McKenzie in 2010, in 8.3 m water depth. The  
93 five centimetre diameter cores (LM1 and LM2) were extracted using a gravity corer, extruded on the  
94 lake edge, and sliced into either 0.25 cm thick (LM1) or 1 cm thick (LM2) samples. Total un-extruded

95 core length was measured at five to ten centimetre intervals during sampling to monitor any loss of  
96 core recovery. Samples were placed in individual plastic zip-lock bags before being transported and  
97 stored in laboratory freezers.

98 The cores were composed of uniformly dark organic-rich mud, with no visible alterations in  
99 colour or texture. With the exception of one large wood fragment recovered from core LM1,  
100 terrestrial plant macrofossils, such as leaves or seeds, were not encountered in the cores. For this  
101 reason, and in order to target terrestrially-derived carbon, pollen residues were prepared for AMS  
102  $^{14}\text{C}$  dating. Preparation of pollen residues for AMS  $^{14}\text{C}$  dating involved sieving to collect a 10-150  $\mu\text{m}$   
103 size fraction, separation by heavy liquid flotation (LST; SG = 1.8) and treatment with NaOH (10%), HCl  
104 (10%) and  $\text{H}_2\text{SO}_4$  (98%). Pre-treatment of the wood fragment involved acid-alkali-acid treatment and  
105 all samples were graphitised according to standard procedure at the Australian Nuclear Science and  
106 Technology Organisation (ANSTO) (Hua et al., 2001). Radiocarbon dates were calibrated using the  
107 IntCal09 calibration curve (Reimer et al. 2009). Calibrated ages in the text are followed with a 'cal kyr  
108 BP' post-fix, single calibrated dates mentioned in the text refer to the median age in the 2 $\sigma$   
109 calibrated age-range.

110 Abundance of atmosphere-derived  $^{210}\text{Pb}$  ( $^{210}\text{Pb}_{\text{unsupported}}$ ) in the upper sediment was used to  
111 estimate recent sediment accumulation rates at Lake McKenzie. The method, which has been  
112 described in detail by Appleby and Oldfield (1978), Appleby and Oldfield (1992) and Appleby (2001),  
113 uses down-core change in  $^{210}\text{Pb}_{\text{unsupported}}$  activity to calculate an accumulation rate based on the  $^{210}\text{Pb}$   
114 half-life of  $22.26 \pm 0.22$  years.  $^{210}\text{Pb}_{\text{unsupported}}$  was estimated by subtracting activity of supported  $^{210}\text{Pb}$   
115 ( $^{210}\text{Pb}_{\text{supported}}$ ), which was measured indirectly from its grandparent radioisotope Radium-226 ( $^{226}\text{Ra}$ ),  
116 from total  $^{210}\text{Pb}$  ( $^{210}\text{Pb}_{\text{total}}$ ) activity, which was measured indirectly from its progeny polonium-210  
117 ( $^{210}\text{Po}$ ). Both the CIC (constant initial concentration) and the CRS (constant rate of supply) models  
118 (Appleby and Oldfield 1978; Appleby 2001) were applied and calendar ages estimated.

119  $^{210}\text{Pb}_{\text{supported}}$  and  $^{210}\text{Pb}_{\text{total}}$  were measured in the upper 8.5 cm of core LM1. Between 0.18 and 1.23  
120 g of sediment was prepared by heating the samples in  $\text{HNO}_3$  at  $60^\circ\text{C}$ . Once evaporated, small  
121 amounts of  $\text{H}_2\text{O}_2$  (10%) were added with heating until the reaction subsided. The samples were  
122 evaporated again before refluxing in a mixture of  $\text{HNO}_3$  and  $\text{HCl}$  (1:3;  $50\text{--}60^\circ\text{C}$ ) for at least 4 hours.  
123 Samples were subsequently redissolved in  $\text{HCl}$  (6M) and centrifuged to separate the supernatant  
124 from the residue. The supernatant was collected and processed to remove excess iron by diethyl  
125 ether solvent extraction.  $^{210}\text{Po}$  and  $^{209}\text{Po}$  were isolated by auto-deposition onto silver discs using  
126  $\text{NH}_2\text{OH}\cdot\text{HCl}$ .  $^{226}\text{Ra}$  and  $^{133}\text{Ba}$  were isolated by co-precipitation and collected as colloidal micro-  
127 precipitates on  $0.1\ \mu\text{m}$  Millipore VV membrane filters. The recovery of the preparation method was  
128 assessed using radioactive tracers  $^{133}\text{Ba}$  ( $\sim 85\ \text{Bq}$ ) for  $^{226}\text{Ra}$  recovery and  $^{209}\text{Po}$  ( $\sim 0.2\ \text{Bq}$ ) for  $^{210}\text{Po}$   
129 recovery, which were added at the start of the sample processing procedure. The auto-plated  
130 polonium on the silver discs and the radium micro-precipitates on membrane filters were analysed  
131 using ORTEC alpha spectrometers to determine  $^{210}\text{Po}$  and  $^{226}\text{Ra}$  activities.  $^{133}\text{Ba}$  was analysed using a  
132 HPGE gamma spectrometer.

133

#### 134 Microfossil analysis

135 Thirty-two samples from core LM2 were prepared for microfossil analysis. This preparation involved  
136 sieving using a  $125\ \mu\text{m}$  mesh, treatment with  $\text{HCl}$  (10%),  $\text{KOH}$  (10%),  $\text{HF}$  (40%), acetolysis and  
137 mounting in glycerol. A known quantity of *Lycopodium* marker grains was added to each sample to  
138 allow for quantification of microfossils. Microfossils were counted under an Olympus BX50  
139 microscope at  $600\times$  magnification and pollen was counted until 300 grains of terrestrial plant types  
140 were observed. Pollen identification was assisted by online resources (Newcastle Pollen Collection  
141 2002; Australasian Pollen and Spore Atlas 2013) and published literature (Pike 1956). Results are  
142 presented as percentages of the total terrestrial pollen sum. Pollen zones were assigned on the basis

143 of a stratigraphically constrained cluster analysis (CONISS) (Grimm 1987) performed using Tilia  
144 software (v. 1.7.16) (Grimm 1992).

145 Micro-charcoal particle and *Botryococcus* colony concentrations were estimated using the point  
146 count method (Clark 1982). Micro-charcoal particles were identified based on their black or  
147 transparent grey colour and jagged outline and only particles with an axis longer than 10 µm were  
148 counted.

149

150 Total organic carbon (TOC), total nitrogen (TN) and bulk organic  $\delta^{13}\text{C}$  and  $\delta^{15}\text{N}$  analysis

151 All samples from core LM2 were analysed on a Delta V Advantage Continuous Flow Isotope Ratio  
152 Mass Spectrometer-Flash 2000 HT Elemental Analyser for C%, N%,  $\delta^{13}\text{C}$  and  $\delta^{15}\text{N}$ . Nitrogen  
153 measurements were conducted on oven dried (40 °C), homogenised sediment. Carbon  
154 measurements were conducted on the same aliquots after they had been treated with HCl (10%) to  
155 remove any carbonate material present in the sample. The reference materials used were:  $\text{CO}_2$  -  
156 calibrated against IAEA CH6 with a consensus value of 10.449‰ Vienna Peedee Belemnite (VPDB)  
157 (Coplen et al. 2006);  $\text{N}_2$  - calibrated against IAEA N-1 with a consensus value of  $\delta^{15}\text{NAIR} = +0.4\text{‰}$   
158 (Bohlke and Coplen, 1995); working soil standard AILS SSA (ANSTO Isotope Laboratory Standard -  
159 Simulated Soil Aliquot); and acetanilide. The results are reported relative to VPDB for C and air for N.

160

161 Lipid analysis

162 Twelve samples from core LM2 were extracted using a Soxhlet apparatus and pre-extracted cellulose  
163 thimbles. Extractions were performed on 3-5 g of dried and ground sediment for 24 hours, with a  
164 solvent mixture of dichloromethane and methanol (9:1). Activated copper turnings were added to  
165 the collection flask to remove elemental sulphur. Extracts were separated into two aliquots,

166 evaporated to dryness and weighed. Aliquots of each sample were initially prepared for GC-MS  
167 analysis using the separation procedure described below. A modified separation procedure was then  
168 performed on remaining aliquots of 6 samples, prior to analysis by isotope ratio monitoring (irm)-  
169 GC-MS.

170 Aliquots of extracts were initially separated using a small column (50 mm x 5 mm) filled with  
171 activated silica gel pre-eluted with *n*-Hexane. Extracts were progressively eluted with 2 ml of  
172 *n*-Hexane (the saturated hydrocarbon fraction), 3:7 DCM: *n*-Hexane (the aromatic hydrocarbon  
173 fraction) and 1:1 DCM: *n*-Hexane (the polar fraction). Known volumes of squalane (Fluka 85629)  
174 were added to the saturated hydrocarbon fractions to allow for estimation of compound  
175 concentrations. A modified separation procedure was performed on samples prior to irm-GC-MS  
176 analysis in order to improve compound separation. Extracts were added to the top of a large column  
177 (20 cm x 1 cm) filled with activated silica gel and eluted progressively with *n*-Pentane (2 bed-loads;  
178 'F1' fraction); 3:7 DCM: *n*-Pentane (2 bed-loads; 'F2' fraction); and 1:1 DCM: *n*-Pentane (2 bed-loads;  
179 'F3' fraction). Fractions 'F1' and 'F2' were combined and re-separating using a small column (50 mm x  
180 5 mm) and eluted with *n*-Hexane (1 bed-load; 'F1a' fraction); *n*-Hexane (2 bed-loads; 'F1b' fraction);  
181 *n*-Hexane (2 bed-loads; 'F1c' fraction); and 1:1 DCM: Methanol (2 bed-loads; 'F2' fraction). Aliphatic  
182 and aromatic fractions were analysed by GC-MS. In some cases individual fractions were combined  
183 prior to measurement by irm-GC-MS, in order to completely capture compounds that eluted across  
184 fractions.

185 GC-MS analysis used a Hewlett Packard (HP) 5973 mass selective detector interfaced to HP 6890  
186 gas chromatograph, fitted with a DB-5MS column (60 m x 0.25  $\mu\text{m}$  i.d.; J and W Scientific). The GC  
187 oven was programmed to increase from 40 °C to 300 °C at 3 °C  $\text{min}^{-1}$  with an initial hold time of 1  
188 minute and a final hold time of 30 min. Samples were dissolved in *n*-Hexane and injected on-column  
189 using a HP 6890 auto-sampler. Helium was used as the carrier gas, at a linear velocity of 28  $\text{cm s}^{-1}$   
190 and the injector operating at constant flow. Typically the MS was operating at an ionisation energy



191 of 70 eV, a source temperature of 180 °C, with an electron multiplier voltage of 1800 V and a mass  
192 range of 50 to 550 amu.

193 Compound specific carbon isotope ratios were measured on an HP 6890 GC equipped with a  
194 HP6890 autosampler and interfaced to an Isoprime Micromass isotope ratio monitoring mass  
195 spectrometer. GC conditions were identical to those for GC-MS analysis described above. Each  
196 sample was analysed at least twice and  $\delta^{13}\text{C}$  values are reported relative to VPDB. Maximum  
197 deviation between separate analyses was less than or equal to 0.5‰ for all but 7 of the biomarker  
198  $\delta^{13}\text{C}$  values reported here. Standard mixes with compounds of known isotope values were run at  
199 least between every two samples in order to monitor the stability of the system.

200

## 201 **Results**

### 202 Age model

203 The age model for Lake McKenzie has been previously described by Woltering et al. (2014) and was  
204 based on a deposition model that was constructed using OxCal (version 4.1) (Bronk Ramsey 2008,  
205 2009) (Fig. 2). The deposition model excluded three dates that appeared to be outlying (OZN680,  
206 OZN681 and OZO411). Two of those dates (OZN680 and OZN681) were obtained at the same depth  
207 on core LM1, and appear to mark a sedimentary disturbance which may be related to the presence  
208 of the wood fragment. The third date relates to an age reversal of 1970  $^{14}\text{C}$  years which occurs  
209 between dates at 20-21 and 23-24 cm depths. In the absence of an obvious reason to exclude either  
210 date from the deposition model, Oxcal overall Agreement Indexes and Oxcal Outlier Analyses were  
211 compared to determine which had a higher likelihood of being erroneous. A low overall Agreement  
212 Index was produced when OZN685 excluded in a P\_Sequence deposition model (58.2%), compared  
213 to that produced when OZO411 was excluded (65.3%), and Outlier Analyses indicated a higher  
214 posterior probability of OZO411 being an outlier compared with OZN685. Thus OZO411 was deemed  
215 to be a more likely outlier, and was excluded from the deposition model.

216 The sediment cores lacked visible lithological changes, however a large age difference of ca. 4.3 kyr  
217 was observed between contiguous samples obtained from 25-26 and 26-27 cm depths (OZN686 and  
218 OZ0412). Despite any visible indication of a break in sediment accumulation, the radiocarbon dates  
219 suggest a slowing or ceasing of sediment accumulation in the time interval of ca. 18.3-14.0 cal kyr  
220 BP.

221 Geochemical analyses

222 Marked changes in TOC%, TOC/TN and bulk organic matter  $\delta^{13}\text{C}$  and  $\delta^{15}\text{N}$  occur with depth (Fig. 3)  
223 and are characterised by a down-core increase in TOC/TN and decrease in  $\delta^{15}\text{N}$  values. Nine  
224 compounds were observed that have been identified as botryococcenes (Fig. 4; Supplementary  
225 Material). Their identification was based on comparisons with published mass spectra of  
226 botryococcene compounds and Kováts indexes (Huang et al. 1999; Gao et al. 2007; de Mesmay et al.  
227 2008). Botryococcenes from Lake McKenzie were also compared with a sample containing a  
228 compound previously identified as 1, 6, 17, 21-octahydrobotryococcene by Huang et al. (1999). A  
229 good match in elution time and mass spectra was found between this sample and the compound  
230 described here as the **A2** botryococcene. With the exception of the **C0** botryococcene, all  
231 botryococcenes display higher concentrations in the lower samples, below 26 cm depth (Fig. 3). The  
232 **C0** botryococcene however, shows a distinct down-core trend: concentrations of this compound  
233 peak at 17 cm and are low below 26 cm. Botryococcene compounds were observed to have  $\delta^{13}\text{C}$   
234 values in the range of -31.7‰ to -22.5‰ (Table 3).

235 Long chain *n*-alkanes observed in the Lake McKenzie samples had a strong odd-over-even  
236 predominance (Fig. 4) and had average chain lengths (C25- C33) between 27.6 and 29.1. Chain  
237 length was observed to increase with depth.  $\delta^{13}\text{C}$  values of odd C23-C33 *n*-alkanes ranged  
238 from -38.6‰ to -30.3‰ (Table 3). A C<sub>20</sub> HBI was also observed in the samples and showed higher  
239 concentrations in the upper samples and had a maximum concentration at 10 cm depth (Fig. 3).

240

241 Microfossil analyses

242 The pollen diagram for Lake McKenzie is presented in Figure 5. A depth constrained cluster analysis  
243 (CONISS) was performed using all pollen types in order to identify pollen zones (Grimm 1987);  
244 characteristics of each pollen zone are described below.

245

246 *Pollen zone LM2-1: 46-34 cm depth, ca. 36.9-26.9 cal kyr BP*

247 Pollen zone LM2-1 is characterised by high proportions of terrestrial herb pollen (mean = 15.3%), of  
248 which Poaceae pollen is of highest abundance (11.1%), and is followed by *Amperea* (1.6%) and  
249 Asteraceae (Tubuliflorae) (1.3%). Percentages of aquatic/littoral pollen are moderately high through  
250 most of this zone (9.6%), and are dominated by Cyperaceae and Restionaceae. Casuarinaceae pollen  
251 dominates the arboreal taxa (42.5%) and of the Myrtaceae pollen identified to genus level,  
252 *Eucalyptus* and *Melaleuca* dominate. Moderate concentrations of micro-charcoal occur (195.9 cm<sup>2</sup>  
253 g<sup>-1</sup>). Concentrations of *Botryococcus* colonies are high (323.6 cm<sup>2</sup> g<sup>-1</sup>) compared to the overlying  
254 zones.

255

256 *Pollen zone LM2-2: 34-26 cm depth, ca. 26.9-18.3 cal kyr BP*

257 Pollen zone LM2-2 is characterised by high percentages of pollen from aquatic/littoral plants (17.3%)  
258 and relatively high percentages of terrestrial herb pollen (14.5%). Highest percentages of *Typha*  
259 pollen occur in this zone (5.3%) and a sharp peak in *Typha* occurs at 33 cm depth. Cyperaceae also  
260 occurs in high abundance (8.5%). A gradual replacement of Casuarinaceae with Myrtaceae pollen  
261 occurs up-core through this zone. Terrestrial herb pollen is dominated by Poaceae (9.9%) and to a  
262 lesser degree Asteraceae (Tubuliflorae) (1.6%), Chenopodiaceae (1.3%) and *Amperea* (0.8%).

263 Concentrations of micro-charcoal are high in this zone ( $519.9 \text{ cm}^2 \text{ g}^{-1}$ ), peaking at 27 cm depth.

264 *Botryococcus* colonies remain abundant ( $291.9 \text{ cm}^2 \text{ g}^{-1}$ ).

265

266 *Hiatus: 26-25 cm depth, ca. 18.3-14.0 cal kyr BP*

267 An age difference of ca. 4.3 kyr is observed between contiguous samples taken from 25-26 and 26-

268 27 cm depth. Although no lithological change occurs at this depth, the AMS  $^{14}\text{C}$  dates suggest a

269 hiatus is present spanning the time period from ca. 18.3-14.0 cal kyr BP.

270

271 *Pollen zone LM2-3: 25-18 cm depth, ca. 14.0-6.1 cal kyr BP*

272 A large change in the microfossil assemblage marks the lower boundary of this pollen zone. At the

273 commencement of this zone, pollen of aquatic/littoral taxa are markedly reduced compared with the

274 underlying zone (3.1%), as is Poaceae pollen (2.1%) and concentrations of both micro-charcoal ( $90.7$

275  $\text{cm}^2 \text{ g}^{-1}$ ) and *Botryococcus* colonies ( $39.2 \text{ cm}^2 \text{ g}^{-1}$ ). Casuarinaceae pollen dominates the arboreal

276 pollen (45.7%), and of the myrtaceous pollen types, *Lophostemon* and *Callistemon* are increased

277 compared with the underlying zone (respectively 2.3% and 4.7%), while *Acmena* is decreased (0.2%).

278 Percentages of *Monotoca* are higher (7.8%), while percentages of Asteraceae (Tubuliflorae) and

279 Chenopodiaceae pollen are lower (respectively 0.2% and 0.4%) than the underlying zone.

280

281 *Pollen zone LM2-4: 18-10 cm depth, ca. 6.1-2.5 cal kyr BP*

282 Pollen zone LM2-4 is characterised by having the highest percentages of Myrtaceous pollen (59.6%).

283 Percentages of Moraceae (0.5%) and *Dodonaea* (1.2%) are slightly increased compared with the

284 underlying zones. Percentages of Casuarinaceae pollen are low (19.2%) while Myrtaceae pollen is

285 high (59.1%). Pollen from aquatic/littoral taxa is slightly more abundant in this zone (3.7%) and two

286 peaks in their abundance occur at 15 and 10 cm depth. Micro-charcoal and *Botryococcus*  
287 concentrations also show slight increases around 15 and 10 cm depth, but on the whole are low in  
288 this zone. Percentages of Poaceae pollen are increased slightly (2.9%), compared with the underlying  
289 zone.

290

291 *Pollen zone LM2-5: 10-0 cm depth, ca. 2.5-0 cal kyr BP*

292 The uppermost pollen zone is characterised by reduced percentages of aquatic/littoral pollen (1.8%)  
293 and high percentages of *Monotoca* (12.6%). Casuarinaceae pollen is more abundant compared with  
294 the underlying zone (29.0%), as is *Dodonaea* (2.8%) and *Eucalyptus* (15.3%). Concentrations of  
295 micro-charcoal and *Botryococcus* colonies are slightly increased compared with the underlying zone  
296 (respectively 92.1 and 59.0 cm<sup>2</sup> g<sup>-1</sup>), and show a small increase around 4 cm depth. Pollen from *Pinus*  
297 increases markedly at 4 cm depth.

298

## 299 **Discussion**

300 Chronological assessment of the Lake McKenzie record

301 Obtaining reliable radiocarbon age estimates on organic remains from lake sediments can be  
302 problematic, as lake sediments are susceptible to producing dates that appear greater than the date  
303 of sediment deposition. Processes leading to erroneously old radiocarbon ages commonly arise  
304 when organic matter that is depleted in <sup>14</sup>C in relation to the contemporaneous atmosphere is  
305 incorporated into the sediments *via* dissolved forms of carbon, or *via* organic remains transported to  
306 the lake after a period of storage in the catchment (Bjorck and Wohlfarth 2001; Walker et al. 2007).

307 Terrestrial plant remains are preferentially selected for radiocarbon dating as those remains are  
308 unaffected by lake water reservoir effects, and when those remains are relatively fragile they are

309 unlikely to withstand sediment reworking and long term storage processes in the catchment. They  
310 thus have a  $^{14}\text{C}$  composition that is consistent with the atmosphere contemporaneous to sediment  
311 deposition (Bjorck and Wohlfarth 2001; Walker et al. 2007). A lack of suitable terrestrial macrofossils  
312 in the Lake McKenzie cores led to pollen residues being targeted for radiocarbon dating. Pollen is an  
313 advantageous material as it is primarily of terrestrial origin, it often has a short transport time from  
314 site of production, and is commonly abundant in lake sediments (Vandergoes and Prior 2003).  
315 However, prepared pollen fractions typically contain some organic detritus of unknown sources, and  
316 this potentially influences radiocarbon age estimates (Bjorck and Wohlfarth 2001). And as pollen  
317 exines are robust, pollen can be stored for lengthy periods of time on catchment slopes prior to  
318 being deposited in lake sediments and thus potentially incorporate a time lag into radiocarbon age  
319 estimates. At Lake McKenzie, the proportion of pollen transported to the lake *via* surface runoff is  
320 minimised by the lack of inflowing water channels. Additionally, the lake catchment has been  
321 predominantly vegetated with forest or woodland, and thus major events of sediment input would  
322 be largely restricted to periods following vegetation disturbance, after severe fire or storm, for  
323 example. Therefore time lags associated with sediment storage prior to deposition are unlikely to be  
324 a major influence on age estimates at Lake McKenzie.

325 The exact reason for the observed slow rate of sediment accumulation at Lake McKenzie is  
326 difficult to determine. Physical and chemical characteristics of Lake McKenzie are distinctly different  
327 to Lake Allom and Hidden Lake, where faster rates of sediment accumulation have been reported  
328 (Longmore 1998; Donders et al. 2006). Comparable rates of sediment accumulation are reported at  
329 Old Lake Coomboo Depression (Longmore and Heijnis 1999) and both Lake McKenzie and Old Lake  
330 Coomboo Depression are similar in the sense that they have relatively flat lake bed topographies, as  
331 opposed to Hidden Lake which has steeper slopes. While Lake McKenzie, Lake Allom and Hidden  
332 Lake are all oligotrophic and acidic (pH 4.0-5.8), Lake McKenzie has markedly clearer water, and  
333 lower Total Phosphorus ( $\leq 5 \mu\text{g l}^{-1}$ ), Total Nitrogen ( $\leq 70 \mu\text{g l}^{-1}$ ) and Chlorophyll-a ( $\leq 0.2 \mu\text{g l}^{-1}$ ) content  
334 (Bowling 1988; Longmore 1998; Hadwen et al. 2003). These parameters may be related to a low rate

335 of lake productivity or high rate of sediment diagenesis, and thus a slower sediment accumulation  
336 rate at Lake McKenzie. Bioturbation does not appear to have played a major role at the Lake  
337 McKenzie coring site over the last 130 years as a clear monotonic decrease in  $^{210}\text{Pb}_{\text{unsupported}}$  is  
338 observed in the upper part of the record. High water content, and low bulk density (Hembrow et al.  
339 2013) in the upper layers of the sediment may account in part for the observed increase in sediment  
340 accumulation rate above 7 cm depth.

341

342 Environmental conditions at Lake McKenzie from ca. 36.9-18.3 cal kyr BP

343 The combined evidence presented here indicates that during the glacial period Lake McKenzie was  
344 shallow or ephemeral, and had an expanded littoral zone compared to present. Plants of the littoral  
345 or shallow water zone were abundant between ca. 36.9 and 18.3 cal kyr BP, as indicated by the high  
346 proportions of Cyperaceae and Restionaceae pollen in the record. Poaceae abundance is high at this  
347 time, which reflects either expanded grassy openings in surrounding vegetation, or an expanded  
348 littoral zone. The presence of long-chain *n*-alkanes with an odd-over-even predominance and  $\delta^{13}\text{C}$   
349 values within the range of -35.7 to -31.5‰ indicates a major source from terrestrial C3 plants  
350 (Eglinton and Hamilton 1967; Rieley et al. 1991). As do the  $\delta^{13}\text{C}$  values of bulk organic matter which  
351 range from -28.5 to -27.7‰ (Smith and Epstein 1971; Tieszen 1991). High TOC/TN values suggest  
352 emergent and terrestrial plants are a dominant source of organic matter to the lake sediment  
353 (Bianchi and Canuel 2011), however caution in the interpretation of TOC/TN ratios is required at  
354 Lake McKenzie as *Botryococcus braunii* is known to produce bulk organic matter with high values.  
355 TOC/TN ratios greater than 20 have previously been observed for the algal colonies (Grice et al.  
356 1998, 2001; Huang et al. 1999).

357 The green colonial alga *Botryococcus braunii* is the likely source of the botryococcene compounds  
358 observed in the Lake McKenzie sediments (Maxwell et al. 1968; Metzger et al. 1991). Down-core

359 changes in abundance of botryococccenes and microfossils of *Botryococcus* show similar variation  
360 (Fig. 3 and 5), with highest abundance of both proxies occurring in two separate periods, at around  
361 36.0-30.8 cal kyr BP and 23.5-20.3 cal kyr BP. The reason for the high abundance of *Botryococcus*  
362 during the glacial period is not known, but could be linked to factors such as the nutrient status of  
363 the lake water, or the presence of other phytoplankton with faster growth rates at the site. These  
364 factors influence the modern distribution of the algae (Cook et al. 2011). The lower atmospheric CO<sub>2</sub>  
365 partial pressure of the glacial period would presumably have been favourable to this green alga, as it  
366 has a CO<sub>2</sub> concentrating mechanism (Street-Perrott et al. 1997; Huang et al. 1999). The modern  
367 distribution of *Botryococcus* is broad and the alga appears to have a wide ranging environmental  
368 tolerance, however the alga is most commonly observed in freshwater oligotrophic lakes and ponds  
369 (Cook et al. 2011) and its presence has previously been used to understand past changes in  
370 eutrophication resulting from human activity (Smittenberg et al. 2005).

371 Botryococcene  $\delta^{13}\text{C}$  values for the glacial period of the record range from -31.7‰ to -22.5‰ and  
372 this is within the range of botryococccenes observed in Quaternary lake sediments at other sites (e.g.  
373 Grice et al. 1998; Huang et al. 1999; Smittenberg et al. 2005; Gao et al. 2007; Grossi et al. 2012). This  
374 large range in  $\delta^{13}\text{C}$  values is seen in a single sample from 27 cm depth (Table 3). Wide and  
375 contemporaneous variation in  $\delta^{13}\text{C}$  values of botryococccenes has previously been observed, and  
376 suggested to derive from their synthesis during successional periods of an algal bloom, when lake  
377 water characteristics such as dissolved nutrients, pH and dissolved CO<sub>2</sub> were undergoing alteration  
378 (Huang et al. 1999). This is a potential cause for the wide range in  $\delta^{13}\text{C}$  values observed within the  
379 one centimetre thick samples from the Lake McKenzie core.

380 Although the number of  $\delta^{13}\text{C}$  values obtained on individual botryococcene compounds from Lake  
381 McKenzie is small, a  $\delta^{13}\text{C}$  maximum occurs in zone LM2-2 (ca. 26.9 - 18.3 cal kyr BP) (Table 3), and  
382 this  $^{13}\text{C}$  enrichment is also observed in the C29, C31 and C33 *n*-alkanes from this zone. The timing of  
383 this apparent carbon isotope excursion corresponds with the terminal period of the last glacial and a



384 similarly timed positive shift in botryococcene  $\delta^{13}\text{C}$  values has previously been observed in a lake  
385 record from Mt Kenya (Huang et al. 1999). While the magnitude of the shift is greater in the Mt  
386 Kenya record, the proposed cause for the isotopic shift at that site, from the depletion of  $\text{CO}_2(\text{aq})$   
387 under the lower atmospheric  $p\text{CO}_2$  of the LGM, may also explain the observed shift to more positive  
388 botryococcene  $\delta^{13}\text{C}$  values at Lake McKenzie.

389 Cooler conditions at Lake McKenzie during the glacial are suggested by the slightly higher  
390 abundance of Asteraceae (Tubuliflorae). Previous work on GDGT distributions at Lake McKenzie,  
391 using a global soil calibration, estimated mean annual air temperature to have been 4.1 °C cooler at  
392 the site around 18.8 cal. kyr BP compared to present (Woltering et al. 2014).

393 Micro-charcoal particles are abundant during the glacial period of the record and reflect a higher  
394 frequency and/or intensity of burning, probably as a result of dryer conditions. The influence of  
395 humans on fire activity at Lake McKenzie during the glacial period is difficult to discern however. The  
396 record does not extend far enough into the past to capture the initial occupation of the Australian  
397 continent, and the record does not contain information about short-term alterations in fire activity,  
398 as the time resolution for each sample is low. The presence of humans in SEQ during the glacial  
399 period is confirmed by the occupation of Wallen Wallen Creek site on North Stradbroke Island  
400 around 21,800  $^{14}\text{C}$  yr BP (Neal and Stock 1986; Ulm 2011). However, very little is known about pre-  
401 Holocene human occupation of this area, as an extremely low number of archaeological sites have  
402 been discovered (Bowdler 2010). In a continent that was dryer, windier and cooler than present  
403 (Harrison and Dodson 1993; Hesse et al. 2004; Williams et al. 2009), resources available on Fraser  
404 Island - from perched lakes, swamps and rainforest refugia for example – would seemingly have  
405 been attractive to people. However further archaeological work is required to understand the extent  
406 of human-induced fire activity on Fraser Island and on the nearby mainland.

407

408 Deglaciation

409 The observed ceasing or slowing of sediment accumulation at Lake McKenzie during deglaciation (ca.  
410 18.3-14.0 cal kyr BP) is likely to have been caused by the lake becoming perennially or intermittently  
411 dry. Perched lake sediments are prone to hiatuses, due to their sensitivity to change in precipitation  
412 and evaporation (Verschuren 2003). A hiatus is reported in the Lake Allom record, persisting to  
413 around 12.0 cal kyr BP (Donders et al. 2006), and while detection of hiatuses in the Old Lake  
414 Coomboo Depression (OLCD) record is restricted by the low frequency of radiocarbon dates, a sandy  
415 layer bounded by radiocarbon dates of ca. 26.0 and 14.5 cal kyr BP has been suggested to indicate  
416 dry conditions (Longmore and Heijnis 1999). Although the presence of hiatuses limits the amount of  
417 information that can be gained, all three of the lake sediment records that extend into the glacial  
418 that are now available from Fraser Island contain evidence of dry conditions occurring between the  
419 time period of ca. 18.3-14.5 cal kyr BP.

420 The timing of dry periods observed in Fraser Island records during deglaciation does not conform  
421 to climate shifts observed on North Stradbroke Island. There, vegetation reconstructions show arid  
422 periods occurring later than those on Fraser Island. The Native Companion Lagoon record shows  
423 evidence of dryer conditions at ca. 13.7 and 10.5 cal kyr BP; at Welsby Lagoon drying appears at ca.  
424 14.0-12.0 cal. yr BP and 11.5 cal. kyr BP; and at Tortoise Lagoon drying appears at 14.0-12.0, 11.8  
425 and 11.0 cal kyr BP (Moss et al. 2013). Higher resolution work in both regions, but particularly on or  
426 near Fraser Island, is required to more precisely understand the timing and synchronicity of  
427 deglaciation climate changes in southeast Queensland. However, as the islands are separated by  
428 more than 1.5 ° of latitude, a time lag in climate shifts occurring in the two areas is feasible given  
429 current understanding about changes that were occurring in offshore marine currents at that time.  
430 According to evidence from marine cores, the zone of separation of the East Australian Current  
431 (EAC) from the Australian continent gradually migrated southwards after the last glacial maximum,  
432 passing Fraser Island and then North Stradbroke Island (Bostock et al. 2006). This current is part of a

433 major circulation system transporting warm tropical waters southwards, and has the effect of  
434 warming ocean water east of Fraser and North Stradbroke Islands. Thus deglaciation change in the  
435 position of this current might have had a non-synchronous influence on precipitation regimes in  
436 southeast Queensland. However other factors, such as differences in the islands' topography or the  
437 effects of sea level rise, may also have affected local moisture regimes of the two regions.

438

439 Environmental conditions at Lake McKenzie since ca. 14.0 cal kyr BP

440 Deeper water conditions at the sampling site from around 14.0 cal kyr BP are suggested by the  
441 reduction in abundance of plants of the littoral and shallow water zones, and the reduced  
442 contribution of terrestrial or emergent plant organic matter in the lake sediments. Wetter conditions  
443 are also suggested by the denser vegetation at the site, indicated by the reduced abundance of  
444 Poaceae and Asteraceae, and reduced fire activity. *Monotoca* and *Lophostemon* are more abundant  
445 during the Holocene and may track the establishment of modern types of eucalypt forest at the site.  
446 Those taxa are abundant in the eucalypt forests that currently occur on the high dunes and sand  
447 plains of Fraser Island, including those surrounding Lake McKenzie (Ryan 2012).

448 Superimposed on the underlying trend of higher effective precipitation during the Holocene is  
449 evidence of a subtle reduction in moisture at the site, commencing around ca. 6.1 cal kyr BP and  
450 persisting to around 2.5 cal kyr BP, suggested by the small increase in littoral plants. This evidence  
451 for dryer conditions commencing around the mid-Holocene is consistent with previous findings from  
452 diatom remains at the site (Hembrow et al. 2013). However unlike the pollen record presented here,  
453 the diatom record showed shallower water conditions persisting to present. Other lake records on  
454 Fraser Island show evidence of dry conditions during the mid-Holocene. At Hidden Lake, a dry period  
455 is reported from ca. 9.5-2.6 cal kyr BP, and is further described as progressing from a period of falling  
456 groundwater levels from ca. 9.5-6.3 cal kyr BP, to stable and low groundwater levels from ca. 6.3-5.1

457 cal kyr BP, and to rising groundwater levels from ca. 5.1-2.6 cal kyr BP (dates are recalibrated using  
458 the original <sup>14</sup>C dates reported by Longmore (1998)). At Lake Allom, dry conditions are the proposed  
459 cause for a sedimentary hiatus spanning from ca. 6.5-5.4 cal kyr BP (Donders et al. 2006), after which  
460 a period of moist conditions and rising lake levels is reported, persisting to ca. 3.0 cal kyr BP. Large-  
461 scale synthesis studies of palaeoclimate records conclude conditions across eastern Australia to have  
462 been more variable or dryer from around 6-5 cal kyr BP, and suggest this to have been due to an  
463 increasing intensity of the El Niño Southern Oscillation (ENSO) (Donders et al. 2007; Petherick et al.  
464 2013; Reeves et al. 2013). As the area of influence of ENSO is wide, its influence on climates of  
465 eastern Australia is expected to have been synchronous (Donders et al. 2007). The return to wetter  
466 conditions in the late Holocene at some Fraser Island sites contrasts with the general trend for  
467 eastern Australia, and suggests that local factors may have been an important influence on the  
468 island's hydrological regimes during the late Holocene.

469 Unlike other botryococenes detected in the Lake McKenzie record, the **CO** botryococene has a  
470 maximum concentration at ca. 5.5 cal kyr BP (Fig. 3). This unique down-core trend of the **CO**  
471 botryococene could be explained by: 1) more than one race of *B. braunii* occurring in the lake over  
472 time; or 2) the same organism synthesising different compounds at different times during the lake's  
473 history. Further work on the alga and its biomarkers is required to determine whether  
474 environmental factors were driving the observed down-core changes in botryococene distributions  
475 at Lake McKenzie.

476 Despite the apparent increase in human occupation of southeast Queensland during the mid-  
477 Holocene (Ulm and Hall 1996; Ulm 2011), evidence of human activity in the form of large shifts in  
478 fire activity or vegetation composition are absent in the Lake McKenzie record. This contrasts with  
479 lake records from parts of North Stradbroke Island where increased burning is detected from the  
480 mid- to late-Holocene and is linked with intensified human activity (Moss et al. 2013). Despite the  
481 absence of human impact evidence in Fraser Island sediment records, archaeological investigations

482 find occupation of the mainland adjacent to Fraser Island to date to at least ca. 5.5 cal kyr BP  
483 (McNiven 1992) and occupation of Fraser Island itself to date to ca. 3 cal kyr BP (Ulm 2011). This  
484 mismatch highlights the need for further palaeoecological and archaeological work to better  
485 understand past human activity in the region.

486

#### 487 **Conclusions**

488 The Lake McKenzie record provides a reconstruction of changes to ecosystem composition occurring  
489 over the last ca. 36.9 cal kyr, inferred from sedimentary micro-fossils, biomarkers and stable isotope  
490 ratios (C and N). Elevated abundance of littoral plants at the site and increased contribution of  
491 allochthonous organic matter to the lake sediment, along with increased abundance of terrestrial  
492 herbs, is interpreted as reflecting sustained dry conditions to at least ca. 18.3 cal kyr BP. The  
493 underlying trend for increasing effective precipitation after ca. 14.0 cal kyr BP is interrupted ca. 6.1  
494 cal kyr BP, when a subtle shift towards dryer conditions is detected in the pollen record. This  
495 conforms to other evidence of mid-Holocene aridity on the island, and in the broader eastern  
496 Australian region. Abundance of both fossil *Botryococcus* colonies and *Botryococcus*-derived  
497 biomarkers indicate that maximum growth of this colonial green alga occurred during the glacial  
498 period, when conditions were drier and cooler, and surrounding vegetation was sparser and more  
499 prone to burning. The evidence presented here for the Lake McKenzie sediment record contributes  
500 to the understanding of spatial and temporal variability of ecological changes occurring on Fraser  
501 Island and in subtropical eastern Australia, and permits a better assessment of the significance of  
502 those ecological shifts in a regional context.

503

#### 504 **Acknowledgements**

505 Janelle Stevenson is thanked for preparing the pollen residues. Linda Barry and Kerry Wilsher are  
506 thanked for assistance associated with sampling. Jack Goralewski and Daniela Fierro are thanked for  
507 undertaking  $^{210}\text{Pb}$  dating, and Fiona Bertuch and Alan Williams are thanked for assisting with AMS  
508  $^{14}\text{C}$  dating. Stephen Clayton and Geoff Chidlow are thanked for technical assistance associated with  
509 GCMS and GC-IRMS measurements. Rene Diocares is thanked for assistance with EA-IRMS  
510 measurements. We thank Lorenz Schwark for helpful discussions about the research project and  
511 Yongsong Huang for generously providing a sample for compound comparison.

512 [Pierre Le Métayer and Kliti Grice were supported by an ARC Discovery grant awarded to Kliti Grice.](#)  
513 [The Australian Nuclear Science and Technology Organisation \(ANSTO\) and The Institute for](#)  
514 [Geoscience Research at Curtin University provided funding for this project.](#)

515

Formatted: Line spacing: Double

516 **References**

- 517 Appleby PG, Oldfield F (1978) The calculation of lead-210 dates assuming a constant rate of supply of  
518 unsupported  $^{210}\text{Pb}$  to the sediment. *Catena* 5: 1-8
- 519 Appleby PG, Oldfield F (1992) Application of  $^{210}\text{Pb}$  to sediment studies. In: Ivonovich M, Harmon RS  
520 (eds) Uranium-series disequilibrium: applications to earth, marine and environmental science.  
521 Oxford University Press, Oxford, pp 731-778
- 522 Appleby PG (2001) Chronostratigraphic techniques in recent sediments. In: Last WM, Smol JP (eds)  
523 Tracking environmental change using lake sediments, Volume 1: Basin analysis, coring and  
524 chronological techniques. Kluwer Academic Publishers, Dordrecht, pp 171-203
- 525 Australasian Pollen and Spore Atlas (2013) Australasian Pollen and Spore Atlas. Canberra, ACT,  
526 Australia. <http://apsa.anu.edu.au/>
- 527 Australian Bureau of Meteorology (2013) Australian Government. <http://www.bom.gov.au/>
- 528 Barr C, Tibby J, Marshall JC, McGregor GB, Moss PT, Halverson GP, Fluin J (2013) Combining  
529 monitoring, models and palaeolimnology to assess ecosystem response to environmental  
530 change at monthly to millennial timescales: the stability of Blue Lake, North Stradbroke Island,  
531 Australia. *Freshwater Biol* 58: 1614-1630
- 532 Bianchi TS, Canuel EA (2011) Chemical biomarkers in aquatic ecosystems. Princeton University Press,  
533 Princeton, New Jersey
- 534 Bjorck S, Wohlfarth B (2001)  $^{14}\text{C}$  chronostratigraphic techniques in paleolimnology. In: Last WM,  
535 Smol JP (eds) Tracking environmental change using lake sediments. Volume 1: Basin analysis,  
536 coring and chronological techniques. Kluwer Academic Publishers, Dordrecht, pp 205-245
- 537 Bohlke JK, Coplen TB (1995) Interlaboratory comparison of reference materials for nitrogen isotope  
538 ratio measurements, taken from an IAEA technical report, References and intercomparison  
539 materials for stable isotopes of light elements. IAEA-TECHDOC-825, September 1995
- 540 Bostock HC, Opdyke BN, Gagan MK, Kiss AE, Fifield LK (2006) Glacial/interglacial changes in the East  
541 Australian current. *Clim Dynam* 26, 645-659
- 542 Bowdler S (2010) The empty coast: conditions for human occupation in southeast Australia during  
543 the late Pleistocene. In: Haberle S, Stevenson J, Prebble M (eds) Altered ecologies: fire climate  
544 and human influence. *Terra Australis* 32. ANU EPress, Canberra, pp 178-186
- 545 Bowling LC (1988) Optical properties, nutrients and phytoplankton of freshwater coastal dune lakes  
546 in south-east Queensland. *Aust J Freshw Res* 39: 805-815
- 547 Bronk Ramsey C (2008) Deposition models for chronological records. *Quat Sci Rev* 27: 42-60
- 548 Bronk Ramsey C (2009) Bayesian analysis of radiocarbon dates. *Radiocarbon* 51: 337-360
- 549 Clark RL (1982) Point count estimation of charcoal in pollen preparations and thin sections of  
550 sediment. *Pollen et Spores* 24: 523-535

- 551 Cook EJ, Van Geel B, Van der Kaars S, van Arkel J (2011) A review of the use of non-pollen  
552 palynomorphs in palaeoecology with examples from Australia. *Palynology* 35: 155-178
- 553 Coplen TB, Brand WA, Gehre, M, Gröning M, Meijer HAJ, Toman B, Verkouteren RM (2006) After two  
554 decades a second anchor for the VPDB  $\delta^{13}\text{C}$  scale. *Rapid Commun Mass Spectrom* 20: 3165-  
555 3166
- 556 de Mesmay R, Metzger P, Grossi V, Derenne S (2008) Mono- and dicyclic unsaturated triterpenoid  
557 hydrocarbons in sediments from Lake Masoko (Tanzania) widely extend the botryococcene  
558 family. *Org Geochem* 39: 879-893
- 559 Donders TH, Wagner F, Visscher H (2006) Late Pleistocene and Holocene subtropical vegetation  
560 dynamics recorded in perched lake deposits on Fraser Island, Queensland, Australia.  
561 *Palaeogeogr, Palaeoclim, Palaeoecol* 241: 417-439
- 562 Donders TH, Haberle SG, Hope G, Wagner F, Visscher H (2007) Pollen evidence for the transition of  
563 the Eastern Australian climate system from the post-glacial to the present-day ENSO mode.  
564 *Quat Sci Rev* 26: 1621-1637
- 565 Eglinton G, Hamilton RJ (1967) Leaf epicuticular waxes. *Science* 156: 1322-1335
- 566 Eglinton TI, Eglinton G (2008) Molecular proxies for paleoclimatology. *Earth Planet Sci Lett* 275: 1-16
- 567 Gao M, Simoneit BRT, Gantar M, Jaffé R (2007) Occurrence and distribution of novel botryococcene  
568 hydrocarbons in freshwater wetlands of the Florida Everglades. *Chemosphere* 70: 224-236
- 569 Grice K, Schouten S, Nissenbaum A, Charrach J, Sinninghe Damsté JS (1998) A remarkable paradox:  
570 sulfurised freshwater algal (*Botryococcus braunii*) lipids in an ancient hypersaline euxinic  
571 ecosystem. *Org Geochem* 28: 195-216
- 572 Grice K, Audino M, Boreham CJ, Alexander R, Kagi RI (2001) Distribution and stable carbon isotopic  
573 compositions of biomarkers in torbanites from different palaeogeographical locations. *Org*  
574 *Geochem* 32: 1195-1210
- 575 Grimm EC (1987) Coniss: a fortran 77 program for stratigraphically constrained cluster analysis by  
576 the method of incremental sum of squares. *Comput and Geosci* 13: 13-35
- 577 Grimm EC (1992) Tilia and Tilia-graph: pollen spreadsheet and graphics programs. Program and  
578 Abstracts, 8th International Palynological Congress, Aix-en-Provence [France]
- 579 Grossi V, de Mesmay R, Bardoux G, Metzger P, Williamson D, Derenne S (2012) Contrasting  
580 variations in the structure and stable carbon isotopic composition of botryococcenes through  
581 the last glacial-interglacial transition in Lake Masoko (southern Tanzania). *Org Geochem* 43:  
582 150-155
- 583 Hadwen WL, Arthington AH, Mosisch TD (2003) The impact of tourism on dune lakes on Fraser  
584 Island, Australia. *Lakes Reserv: Res and Manag* 8: 15-26
- 585 Harrison S, Dodson JR (1993) Climates of Australia and New Guinea since 18,000 yrs BP. In: Wright Jr  
586 HE, Kutzbach JE, Webb III T, Ruddiman WF, Street-Perrott FA, Bartlein PJ (eds) *Global climates*  
587 *since the last glacial maximum*. University of Minnesota Press, Minnesota, pp 265-293



- 588 Hembrow S, Taffs KH (2012) Water quality changes in Lake McKenzie, Fraser Island, Australia: a  
589 Palaeolimnological approach. *Aust Geogr* 43: 291-302
- 590 Hembrow S, Taffs K, Atahan P, Parr J, Zawadzki A, Heijnis H (2014) Diatom community response to  
591 climate variability over the past 37,000 years in the sub-tropics of the Southern Hemisphere.  
592 *Sci Total Environ* 468-469: 774-784
- 593 Hesse PP, Magee JW, van der Kaars S (2004) Late Quaternary climates of the Australian arid zone: a  
594 review. *Quat Int* 118-119: 87-102
- 595 Hua Q, Jacobsen GE, Zoppi U, Lawson EM, Williams AA, Smith AM, McGann MJ (2001) Progress in  
596 radiocarbon target preparation at the Antares AMS centre. *Radiocarbon* 43: 275-282.
- 597 Huang Y, Street-Perrott FA, Perrott RA, Metzger P, Eglinton G (1999) Glacial-interglacial  
598 environmental changes inferred from molecular and compound-specific  $\delta^{13}\text{C}$  analyses of  
599 sediments from Sacred Lake, Mt. Kenya. *Geochim Cosmochim Acta* 63: 1383-1404
- 600 Lees B (2006) Timing and formation of coastal dunes in northern and eastern Australia. *J Coast Res*  
601 22: 78-89
- 602 Longmore ME (1997) Quaternary Palynological Records from Perched Lake Sediments, Fraser Island,  
603 Queensland, Australia: Rainforest, Forest History and Climatic Control. *Aust J Bot* 45: 507-526
- 604 Longmore ME (1998) The middle Holocene 'dry' anomaly on the mid-eastern coast of Australia:  
605 calibration of paleowater depth as a surrogate for effective precipitation using sedimentary  
606 loss on ignition in the perched lake sediments of Fraser Island. *Palaeoclimates* 3: 135-160
- 607 Longmore ME, Heijnis H (1999) Aridity in Australia: Pleistocene records of Palaeohydrological and  
608 Palaeoecological change from the perched lake sediments of Fraser Island, Queensland,  
609 Australia. *Quat Int* 57-58: 35-47
- 610 Maxwell JR, Douglas AG, Eglinton G, McCormick A (1968) The botryococcenes – hydrocarbons of  
611 nove structure from the alga *Botryococcus braunii* Kützing. *Phytochemistry* 7: 2157-2171
- 612 McGowan HA, Petherick LM, Kamber BS (2008) Aeolian sedimentation and climate variability during  
613 the late Quaternary in southeast Queensland, Australia. *Palaeogeogr, Palaeoclim, Palaeoecol*  
614 265: 171-181
- 615 McNiven I (1992) Sandblow sites in the Great Sandy Region, coastal southeast Queensland:  
616 implications for models of late Holocene rainforest exploitation and settlement restructuring.  
617 *Qld Archaeol Res* 9: 1-16
- 618 Metzger P, Largeau C, Casadevall E (1991) Lipids and mcaromolecular lipids of the hydrocarbon-rich  
619 microalga *Botryococcus braunii*. *Progress in the chemistry of organic natural products* 57: 1-  
620 70
- 621 Moss PT, Tibby J, Petherick L, McGowan H, Barr C (2013) Late Quaternary vegetation history of North  
622 Stradbroke Island, Queensland, eastern Australia. *Quat Sci Rev* 74: 257-272
- 623 Neal R, Stock E (1986) Pleistocene occupation in the south-east Queensland coastal region. *Nature*  
624 323: 618-621

- 625 Newcastle Pollen Collection (2002) Newcastle Pollen Collection, Newcastle, NSW, Australia.  
626 <http://www.geo.arizona.edu/palynology/nsw/index.html>
- 627 Petherick L, Bostock H, Cohen TJ, Fitzsimmons K, Tibby J, Fletcher MS, Moss P, Reeves J, Mooney S,  
628 Barrows T, Kemp J, Jansen J, Nanson G, Dosseto A (2013) Climatic records over the past 30 ka  
629 from temperate Australia – a synthesis from the OZ-INTIMATE workgroup. *Quat Sci Rev* 74:  
630 58-77
- 631 Pike KM (1956) Pollen morphology of Myrtaceae from the south-west Pacific area. *Aust J Bot* 4: 13-  
632 53
- 633 Queensland Herbarium (2013) Regional Ecosystem Description Database (REDD). Version 6.1  
634 (February 2013). Queensland Department of Science, Information Technology, Innovation and  
635 the Arts: Brisbane
- 636 Reeves JM, Barrows TT, Cohen TJ, Kiem AS, Bostock HC, Fitzsimmons KE, Jansen JD, Kemp J, Krause  
637 C, Petherick L, Phipps SJ (2013) Climate variability over the last 35,000 years recorded in  
638 marine and terrestrial archives in the Australian region: an OZ-INTIMATE compilation. *Quat Sci*  
639 *Rev* 74: 21-34
- 640 Reimer PJ, Baillie MGL, Bard E, Bayliss A, Beck JW, Blackwell PG, Bronk Ramsey C, Buck CE, Burr GS,  
641 Edwards RL, Friedrich M, Grootes PM, Guilderson TP, Hajdas I, Heaton TJ, Hogg AG, Hughen  
642 KA, Kaiser KF, Kromer B, McCormac FG, Manning SW, Reimer RW, Richards DA, Southon JR,  
643 Talamo S, Turney CSM, van der Plicht J, Weyhenmeyer CE (2009) INTCAL09 and Marine 09  
644 radiocarbon age calibration curves, 0-50,000 years cal BP. *Radiocarbon* 51: 1111-1150
- 645 Rieley G, Collier RJ, Jones DM, Eglinton G, Eakin PA, Fallick AE (1991) Sources of sedimentary lipids  
646 deduced from stable carbon-isotope analyses of individual compounds. *Nature* 352: 425-427
- 647 Ryan TS (2012) Technical Descriptions of Regional Ecosystems of Southeast Queensland. Queensland  
648 Herbarium, Brisbane.
- 649 Sachs JP, Pahnke K, Smittenberg R, Zhang Z (2007) Biomarker indicators of past climate. In Elias S  
650 (ed) *Encyclopedia of Quaternary Science*. Elsevier, Amsterdam, pp 19-48
- 651 Smith BN, Epstein S (1971) Two categories of  $^{13}\text{C}/^{12}\text{C}$  ratios for higher plants. *Plant Physiol* 47: 380-  
652 384
- 653 Smittenberg RH, Baas M, Schouten S, Sinninghe Damsté JS (2005) The demise of the alga  
654 *Botryococcus braunii* from a Norwegian Fjord was due to early eutrophication. *The Holocene*  
655 15: 133-140
- 656 Street-Perrott FA, Huang Y, Perrott RA, Eglinton G, Barker P, Khelifa LB, Harkness DD, Olago DO  
657 (1997) Impact of lower atmospheric carbon dioxide on tropical mountain ecosystems. *Science*  
658 278: 1422-1426
- 659 Tieszen LL (1991) Natural variations in the carbon isotope values of plants: implications for  
660 archaeology, ecology, and palaeoecology. *J Archaeol Sci* 18: 227-248
- 661 Timms BV (1986) The coastal dune lakes of eastern Australia. In: De Deckker P, Williams WD (eds)  
662 *Limnology in Australia*. Springer Nederlands, pp 421-432

- 663 Ulm S, Hall J (1996) Radiocarbon and cultural chronologies in southeast Queensland prehistory.  
664 Tempus 6: 45-62
- 665 Ulm S (2011) Coastal foragers on southern shores: marine resource use in northeast Australia since  
666 the late Pleistocene. In: Bicho NF, Haws JA, Davis LG (eds) Trekking the shore: changing  
667 coastlines and the antiquity of coastal settlement. Springer, New York, pp 441-461
- 668 Vandergoes, M.J., Prior, C.A., 2003. AMS dating of pollen concentrates - a methodological study of  
669 late Quaternary sediments from south westland, New Zealand. Radiocarbon 45, 479-491.
- 670 Verschuren D (2003) Lake-based climate reconstruction in Africa: progress and challenges.  
671 Hydrobiologia 500: 315-330
- 672 Walker WG, Davidson GR, Lange T, Wren D (2007) Accurate lacustrine and wetland sediment  
673 accumulation rates determined from <sup>14</sup>C activity of bulk sediment fractions. Radiocarbon 49:  
674 983-992.
- 675 Williams M, Cook E, van der Kaars S, Barrows T, Shulmeister J, Kershaw P (2009) Glacial and deglacial  
676 climatic patterns in Australia and surrounding regions from 35,000 to 10,000 years ago  
677 reconstructed from terrestrial and near-shore proxy data. Quat Sci Rev 28: 2398-2419
- 678 Woltering M, Atahan P, Grice K, Heijnis H, Taffs K, Dodson J (2014) Glacial and Holocene terrestrial  
679 temperature variability in subtropical east Australia: branched GDGT distributions in a  
680 sediment core from Lake McKenzie. Quat Res 82: 132-145
- 681

682 **Table 1** Total <sup>210</sup>Pb, Supported <sup>210</sup>Pb, Unsupported <sup>210</sup>Pb, and particle size results for samples taken  
 683 from core LM1. Calendar age estimates using the CIC and CRS models are shown (Appleby and  
 684 Oldfield, 1978; Appleby, 2001). Both the original depths measured on core LM1 and the  
 685 corresponding depths on core LM2, as estimated using tie-points on Total Organic Carbon (%)  
 686 curves, are shown.

ANSTO ID	Depth Interval measured on core LM1 (cm)	Corresponding depth interval on core LM2 (cm)	Total <sup>210</sup> Pb (Bq kg <sup>-1</sup> )	Supported <sup>210</sup> Pb (Bq kg <sup>-1</sup> )	Unsupported <sup>210</sup> Pb* (Bq kg <sup>-1</sup> )	Particle size ≤62.5 μm (%)	Calculated CIC age (years)	Calculated CRS age (years)
M897	0.00-0.25	0.0-0.7	614 ± 12	14 ± 2	601 ± 12	74.0	5 ± 5	5 ± 2
M898	0.25-0.50	0.7-1.4	491 ± 24	18 ± 2	484 ± 24	74.0	15 ± 5	13 ± 4
M899	1.50-1.75	4.1-4.8	168 ± 6	19 ± 2	150 ± 6	90.0	65 ± 7	64 ± 8
M900	1.75-2.00	4.8-5.5	98 ± 4	15 ± 2	85 ± 5	77.6	75 ± 8	76 ± 9
M901	3.00-3.50	7.0-7.8	31 ± 1	20 ± 2	12 ± 2	83.9	131 ± 14	130 ± 11
M902	4.50-4.75	9.4-9.8	38 ± 1	27 ± 3	11 ± 3	78.9	-	-
M903	4.75-5.00	9.8-10.2	76 ± 4	63 ± 6	13 ± 7	79.9	-	-
N369	6.00-6.25	11.7-12.2	86 ± 4	22 ± 3	67 ± 5	69.9	-	-
N370	6.25-6.50	12.2-12.6	102 ± 5	42 ± 4	62 ± 6	72.5	-	-
N371	7.00-7.25	13.4-13.8	34 ± 2	33 ± 3	1 ± 4	73.3	-	-
N372	7.25-7.50	13.8-14.2	31 ± 2	33 ± 3	not detected	83.5	-	-
N373	8.00-8.25	15.0-15.2	63 ± 3	28 ± 3	36 ± 4	81.5	-	-
N374	8.25-8.50	15.2-15.5	63 ± 3	32 ± 3	32 ± 5	68.7	-	-

687 \*decay corrected to a fixed date

688

689

690

691 **Table 2** AMS <sup>14</sup>C dates and calibrated age ranges for pollen residues and wood samples with depths  
 692 measured on core LM2.

693

Lab code	Depth (cm)	Core	Composition	<sup>14</sup> C age (yrs BP)	Error (1σ)	Calibrated age-range (cal yr BP; 2σ)
OZN683	10-11	LM2	Pollen	2,395	± 35	2,183 - 2,654
OZN684	15-16	LM2	Pollen	3,785	± 35	3,931 - 4,230
OZN685	20-21	LM2	Pollen	6,485	± 50	7,260 - 7,431
OZO411	23-24	LM2	Pollen	4,515	± 40	5,044 - 5,309
OZN686	25-26	LM2	Pollen	12,110	± 70	13,786 - 14,148
OZO412	26-27	LM2	Pollen	15,100	± 70	18,026 - 18,589
OZN687	30-31	LM2	Pollen	18,670	± 100	21,872 - 22,545
OZN688	35-36	LM2	Pollen	23,270	± 120	27,785 - 28,499
OZN689	40-41	LM2	Pollen	30,940	± 190	34,924 - 36,280
OZN690	45-46	LM2	Pollen	31,870	± 180	35,575 - 36,783
OZN680	21.3-21.5	LM1	Pollen	19,150	± 210	22,330 - 23,428
OZN681	21.3-21.5	LM1	Wood	11,470	± 60	13,188 - 13,457

694

695

696

697 **Table 3**  $\delta^{13}\text{C}$  values of *n*-alkanes and botryococcene compounds at different depths in core LM2. The  
 698 maximum per mil deviation of the measurements is shown in brackets below each  $\delta^{13}\text{C}$  value. The  
 699 dash symbol indicates where no data is available.  
 700

Depth (cm)	<i>n</i> -alkane $\delta^{13}\text{C}$ (‰)						Botryococenes $\delta^{13}\text{C}$ (‰)							Zone
	C23	C25	C27	C29	C31	C33	A2	C1	C2	B3	B4	C3	C4	
1-2	-38.6 (0.0)	-36.6 (0.0)	-34.4 (0.4)	-33.0 (0.0)	-33.2 (0.2)	-33.0 (0.0)	-	-	-	-	-	-	-	LM2-5
10-11	-	-	-	-34.1 (0.1)	-33.5 (0.1)	-33.0 (0.0)	-	-	-	-	-	-	-	LM2-4
21-22	-35.4 (0.3)	-34.6 (0.1)	-32.7 (0.4)	-32.2 (0.0)	-32.7 (0.3)	-34.5 (0.0)	-	-	-25.7 (0.4)	-	-	-	-	LM2-3
24-25	-	-35.9 (0.0)	-32.4 (0.4)	-31.3 (1.5)	-31.9 (0.5)	-32.2 (0.3)	-	-24.6 (0.2)	-22.6 (0.2)	-	-	-24.1 (1.2)	-	LM2-3
27-28	-	-35.7 (0.0)	-34.0 (1.5)	-31.5 (1.0)	-	-31.8 (0.2)	-32.0 (1.3)	-23.9 (0.2)	-22.5 (0.7)	-23.1 (0.5)	-24.0 (0.4)	-23.1 (0.2)	-24.5 (0.5)	LM2-2
31-32	-	-35.2 (0.2)	-34.3 (0.1)	-30.3 (0.0)	-31.9 (0.0)	-31.2 (0.2)	-29.8 (0.0)	-23.6 (0.2)	-24.3 (0.2)	-	-23.7 (0.1)	-22.8 (0.2)	-24.6 (0.1)	LM2-2
38-39	-	-	-32.0 (0.7)	-32.7 (0.2)	-32.4 (0.0)	-31.9 (0.1)	-	-26.9 (0.1)	-23.6 (0.0)	-25.1 (0.2)	-26.2 (0.1)	-25.3 (0.2)	-27.2 (0.1)	LM2-1

701

702

703

704 **Figure captions**

705 **Fig. 1** **A** location of the South Eastern Bioregion on the east coast of the Australian continent (red  
706 coloured area). **B** Vegetation map of Fraser Island (Queensland Herbarium, 2013). The white  
707 triangles mark locations of (1) Lake McKenzie; (2) Hidden Lake; (3) Old Lake Coomboo Depression  
708 (OLCD); and (4) Allom Lake.

709  
710 **Fig. 2** Age-depth diagram for Lake McKenzie incorporating AMS  $^{14}\text{C}$  and  $^{210}\text{Pb}$  ages. The IntCal09  
711 calibration curve (Reimer et al., 2009) and the OxCal P\_Sequence program ( $k = 4$ ) (Bronk Ramsey,  
712 2008, 2009) were used to construct the deposition model.

713  
714 **Fig. 3** Diagram showing elemental composition and stable isotope carbon and nitrogen isotope  
715 ratios measured for the Lake McKenzie core LM2. Concentrations of biomarker compounds are also  
716 shown as a sum of the 9 botryococcene compounds observed in the samples, individual  
717 concentrations of two botryococcenes (**A2** and **C0**) and concentrations of the  $\text{C}_{20}$  HBI. The shaded  
718 area indicates the location of the hiatus suggested by radiocarbon ages on contiguous samples.

719  
720 **Fig. 4** Total ion chromatogram of saturate fraction of Lake McKenzie core LM3, from **A**: 1 cm depth  
721 and **B**: 31 cm depth. Filled squares refer to  $n$ -alkanes and the number above the square refers to  
722 their carbon number. Compounds **A2**, **C1**, **C2**, **B3**, **B4**, **C3**, **C4** and **C5** are observed botryococcene  
723 compounds.

724  
725 **Fig. 5** Pollen diagram for Lake McKenzie core LM2. Pollen data is presented as percentages of the  
726 total terrestrial pollen sum; the units for total pollen are grains  $\text{g}^{-1}$ ; and the units for micro-charcoal  
727 and *Botryococcus* are  $\text{cm}^2 \text{g}^{-1}$ .

728

729 **Supplementary Material**

730

731 The Kováts indexes and diagnostic MS ions for botryococcene compounds identified in the Lake

732 McKenzie sediments.

MF	MW	Compound	K.I.	Diagnostic ions in mass spectra (m/z)
C <sub>34</sub> H <sub>66</sub>	474	A2	2765	474 (9), 291 (22), 207 (7), 137 (44), 123 (50), 109 (61), 81 (100)
C <sub>34</sub> H <sub>62</sub>	470	C1	2775	470 (4), 455 (10), 231 (34), 203 (68), 177 (85), 109 (84), 81 (100)
C <sub>34</sub> H <sub>58</sub>	466	C0	2788	466 (3), 285 (7), 231 (11), 177 (100), 149 (40), 123 (79), 95 (78)
C <sub>34</sub> H <sub>64</sub>	472	C2	2800	472 (22), 443 (14), 233 (14), 178 (100), 123 (89), 109 (84), 83 (78)
C <sub>34</sub> H <sub>60</sub>	468	B3	2812	468 (10), 453 (4), 287 (27), 205 (12), 178 (43), 123 (100), 95 (77)
C <sub>34</sub> H <sub>64</sub>	472	B4	2823	472 (17), 443 (14), 233 (17), 178 (96), 164 (40), 83 (100), 57 (98)
C <sub>36</sub> H <sub>66</sub>	498	C3	2924	498 (14), 469 (6), 233 (8), 178 (78), 123 (84), 109 (84), 83 (100)
C <sub>36</sub> H <sub>68</sub>	500	C4	2967	500 (14), 471 (9), 233 (11), 178 (100), 123 (91), 109 (84), 57 (100)
C <sub>37</sub> H <sub>68</sub>	512	C5	3026	512 (14), 483 (5), 233 (8), 178 (81), 123 (81), 109 (77), 83 (100)

733 MF = molecular formula; MW = molecular weight; KI = pseudo Kováts retention index:  $100_n + 100 * [(R_x - R_n) / (R_{n+1} - R_n)]$   
 734 where x = compound of interest, n = carbon number of the nearest n-alkane eluting in front of x on the GC; R = retention  
 735 time. The numbers in brackets following the diagnostic ions are the relative intensity compared to that of the base peak.

736

737

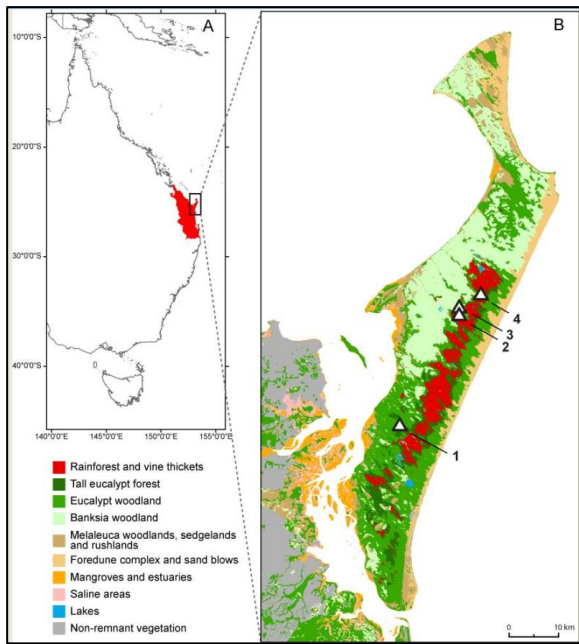


Figure 1

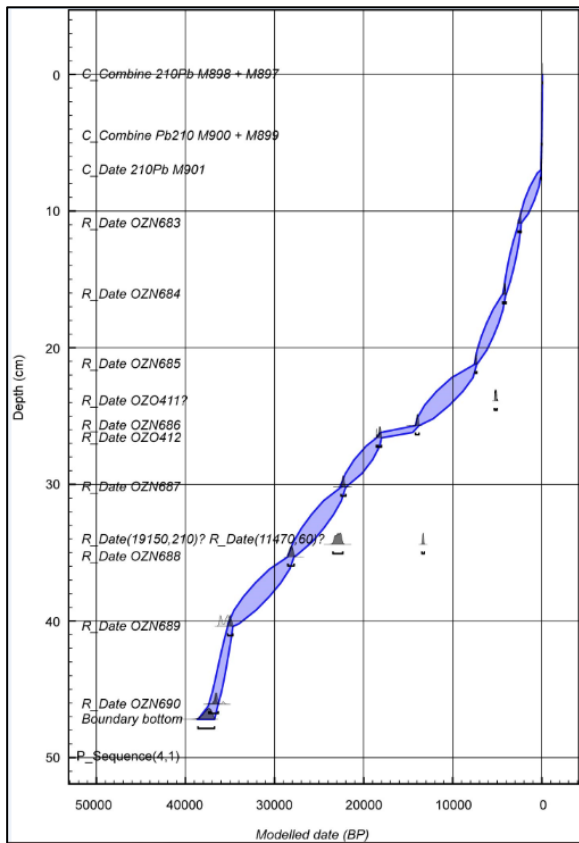


Figure 2



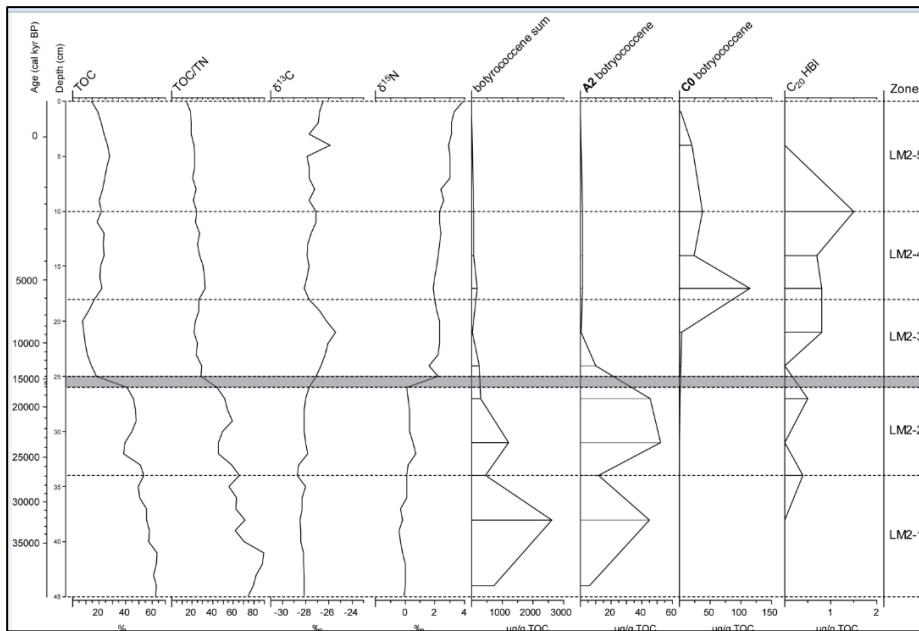


Figure 3

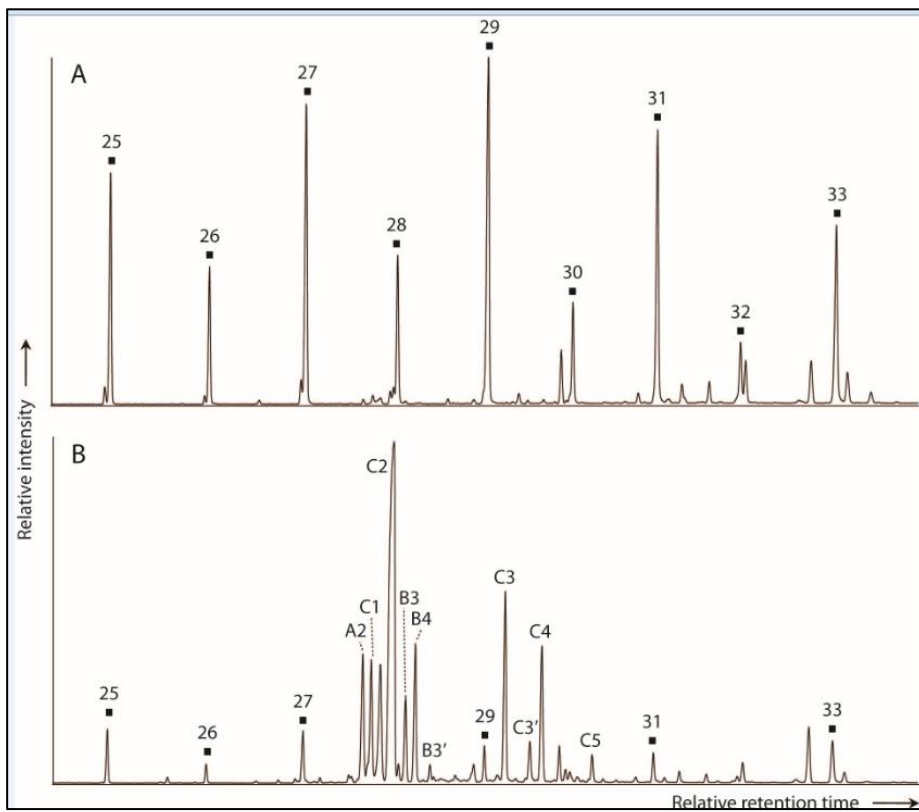


Figure 4

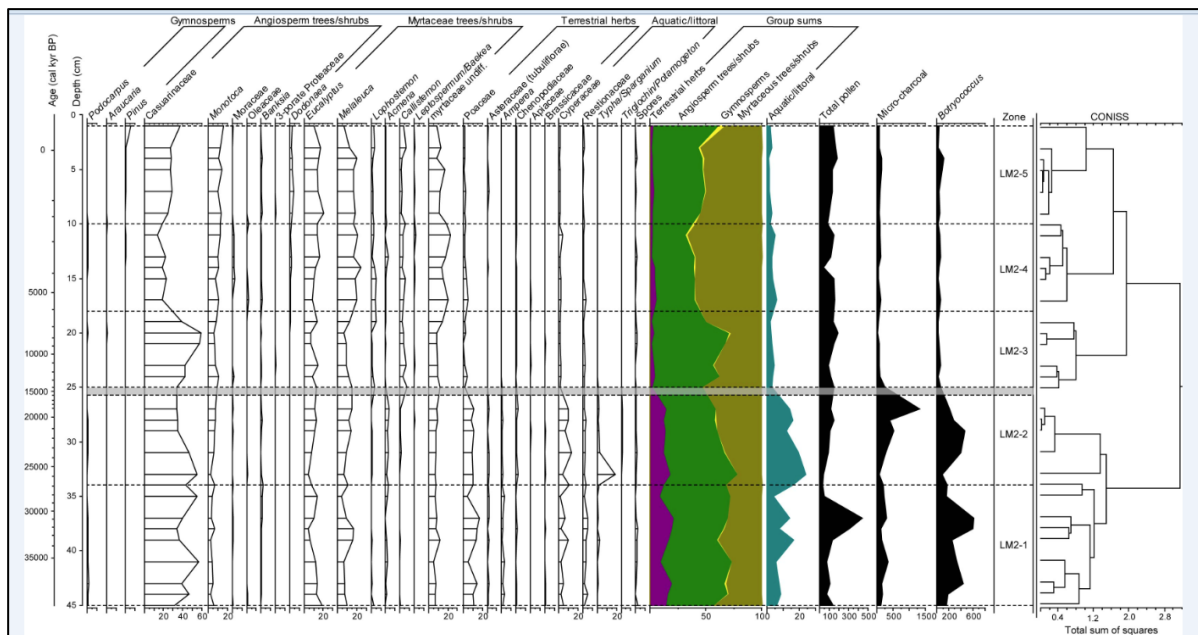


Figure 5